A Numerical Study of Steady Transport Model in Turbulent Flow from a Point Source

Nurcahya Yulian Ashar, and Imam Solekhudin

***Abstract*—In this study, the dispersion of some substance in a river with turbulent flow is considered. In this case, the effect of three factors consist of length, width, and flow velocity on substance dispersion is investigated. The dispersion problem is modeled using diffusion-convection equation. Since the problem may not be solved analytically, a numerical method is chosen, namely the Dual Reciprocity Method (DRM). Numerical solutions are presented to describe the effect of the three factors on the distribution of the substance in the turbulent water flow.**

***Index Terms*—Dual reciprocity method, k-epsilon model, turbulent flow.**

I. Introduction

PROBLEMS related to dispersion of some substanc in a path or medium are usually modeled by the diffusion-convection equation. Samec and Sherget [1] has provided a formula related to the diffusion-convection model. Polyanin [2] and Morales-Delgadoa et. al. [3] studied analytical solutions in certain cases of diffusion-convection problems.

Many of mathematical models may not be solved analytically. Hence, the models need to be solved numerically. Some researchers such as Fajie et. al. [4], Xingxing et. al. [5], Mengxing et. al. [6], and Solekhudin [7] have employed numerical methods for solving diffusion-convection problems. However, none of these researchers consider the problem with point sources. Hence, in this study we consider diffusion-convection problems with a point source.

To solve the diffusion-convection problem with a point source, we employ a Dual Reciprocity Method (DRM). The method may be used to deal with the mathematical term for point sources, which is modelled as Dirac delta functions. This method has been widely used by researchers to solve problems such as heat distribution, infiltration problems and others. Clement and Lobo [9], Solekhudin and Ang [10], Solekhudin [11], Munadi et. al. [12], [13] used DRM to solve infiltration problems from irrigation channels into homogeneous soils. Yun and Ang [14] used DRM to analyze heat distribution in non-homogeneous soils. Ashar [15], and Ashar and Solekhudin [16] has studied the distribution of pollutants for laminar flow. In this paper, DRM is used to observe the behavior of substance dispersion in a single point source on shallow path over turbulent water flow at different lengths, widths, and velocity flow. Solekhudin et al. [17] have employed a DRM for solving infiltration problems into heterogeneous soils.

Manuscript received January 10, 2023; revised August 9, 2023.

Nurcahya Yulian Ashar is a Lecturer at Department of Mathematics, Faculty of Sciences and Mathematics, Universitas Diponegoro, Semarang, 50275 Indonesia. (e-mail: nurcahyayulian@lecturer.undip.ac.id.)

Imam Solekhudin is a Professor at Department of Mathematics, Faculty of Mathematics and Natural Sciences, Universitas Gadjah Mada, Yogyakarta, 55281 Indonesia. (corresponding author, phone: 62-274-552243; e-mail: imams@ugm.ac.id.)

II. Problem formulation and basic equations

In this section, the mathematical model of steady diffusion-convection problems is presented. A brief derivation of DRM for solving the problems is also presented. Steady diffusion-convection problems over a region Π bounded by a simple closed curve Λ are governed by

$$h_1\frac{\partial Z(x,y)}{\partial x}+h_2\frac{\partial Z(x,y)}{\partial y}-C\left(\nabla^2 Z(x,y)\right)=S(x,y), \quad (1)$$

where ∇^2 is $\frac{\partial^2}{\partial x^2}\boldsymbol{i}+\frac{\partial^2}{\partial y^2}\boldsymbol{j}$, Z is substance concentration, h_1 and h_2 are fluid velocity in x and y direction respectively, C is substance diffusion coefficient in fluid, and S is the source. For problems with a point source, the governing equation is

$$\begin{aligned} h_1\frac{\partial Z(x,y)}{\partial x}+h_2\frac{\partial Z(x,y)}{\partial y} &- C\left(\nabla^2 Z(x,y)\right) \\ &= S(x,y)\sigma(x,y;a,b), \quad (2) \end{aligned}$$

where (a,b) is the coordinate of the source, and σ is the Dirac delta function with the source at (a,b). Equation (1) and (2) may be solved numerically using DRM. To solve Equation (1) and (2) using DRM, we first express their solutions in the form of boundary integral equations. The boundary integral equations for Equations (1) and (2) are

$$\begin{aligned} \lambda(\alpha,\beta)\,Z(\alpha,\beta) = & \int_\Lambda \left[Z(x,y)\,\frac{\partial\Theta(x,y;\alpha,\beta)}{\partial n} - \right. \\ & \left. \Theta(x,y;\alpha,\beta)\,\frac{\partial Z(x,y)}{\partial n}\right] ds + \\ & \frac{1}{C}\iint_\Pi \Theta(x,y;\alpha,\beta) \\ & \left[h_1(x,y)\frac{\partial Z(x,y)}{\partial x} + \right. \\ & \left. h_2(x,y)\frac{\partial Z(x,y)}{\partial y} - S(x,y)\right] dx\,dy, \end{aligned} \quad (3)$$

and

$$\begin{aligned}\lambda(\alpha,\beta)\,Z(\alpha,\beta) &= \int_{\Lambda}\left[Z(x,y)\,\frac{\partial\Theta(x,y;\alpha,\beta)}{\partial n} - \right.\\ &\left.\Theta(x,y;\alpha,\beta)\,\frac{\partial Z(x,y)}{\partial n}\right]ds + \\ &\frac{1}{C}\iint_{\Pi}\Theta(x,y;\alpha,\beta)\\ &\left[h_1(x,y)\frac{\partial Z(x,y)}{\partial x} + \right.\\ &\left.h_2(x,y)\frac{\partial Z(x,y)}{\partial y}\right]dx\,dy - \\ &\frac{\Theta(x,y;\alpha,\beta)S(x,y)}{C}, \end{aligned} \tag{4}$$

respectively. Here

$$\lambda(\alpha,\beta) = \begin{cases}1 & ,(\alpha,\beta)\in\Pi\\ \frac{1}{2} & ,(\alpha,\beta)\text{ on the smooth part of }\Lambda,\end{cases}$$

and

$$\Theta(x,y;\alpha,\beta) = \frac{1}{4\pi}\ln\left[(x-\alpha)^2+(y-\beta)^2\right]$$

is the fundamental solution of two-dimensional Laplace's equation. From integral Equations (3) and (4), two systems of linear algebraic equations

$$\begin{aligned}\lambda^{(n)}Z^{(n)} &= \sum_{k=1}^{N}\left[Z^{(n)}\int_{\Lambda^{(k)}}\frac{\partial\Theta\left(x,y;x^{(n)},y^{(n)}\right)}{\partial n}ds - \right.\\ &\left.Z_n^{(k)}\int_{\Lambda^{(k)}}\Theta\left(x,y;x^{(n)},y^{(n)}\right)ds\right] + \\ &\sum_{i=1}^{N+L}\left[h_1^{(n)}\mu_x^{(ni)} + h_2^{(n)}\mu_y^{(ni)}\right]Z^{(i)} - \\ &\sum_{i=1}^{N+L}\mu^{(ni)}S(x^{(i)},y^{(i)})\\ &n = 1,2,\ldots,N+L, \end{aligned} \tag{5}$$

and

$$\begin{aligned}\lambda^{(n)}Z^{(n)} &= \sum_{k=1}^{N}\left[Z^{(n)}\int_{\Lambda^{(k)}}\frac{\partial\Theta\left(x,y;x^{(n)},y^{(n)}\right)}{\partial n}ds - \right.\\ &\left.Z_n^{(k)}\int_{\Lambda^{(k)}}\Theta\left(x,y;x^{(n)},y^{(n)}\right)ds\right] + \\ &\sum_{i=1}^{N+L}\left[h_1^{(n)}\mu_x^{(ni)} + h_2^{(n)}\mu_y^{(ni)}\right]Z^{(i)} - \\ &\Theta(a,b;x^{(n)},y^{(n)})S(a,b),\\ &n = 1,2,\ldots,N+L, \end{aligned} \tag{6}$$

are respectively derived. Here N is the number of segment or element on boundary Λ, segments $\Lambda^{(1)}$, $\Lambda^{(2)}$,..., $\Lambda^{(N)}$ satisfy $\Lambda = \Lambda^{(1)}\cup\Lambda^{(2)}\cup\cdots\cup\Lambda^{(N)}$. Number L is the number of interior collocation point. Points $(x^{(1)},y^{(1)})$, $(x^{(2)},y^{(2)})$, ..., $(x^{(N)},y^{(N)})$ are the midpoints of segments $\Lambda^{(1)}$, $\Lambda^{(2)}$,..., $\Lambda^{(N)}$, respectively. Points $(x^{(N+1)},y^{(N+1)})$, $(x^{(N+2)},y^{(N+2)})$,...,$(x^{(N+L)},y^{(N+L)})$, are the interior collocation points,

$$\begin{aligned}\lambda^{(n)} &= \lambda(x^{(n)},y^{(n)}),\\ Z^{(n)} &= Z(x^{(n)},y^{(n)}),\\ Z_n^{(n)} &= \left.\frac{\partial Z(x,y)}{\partial n}\right|_{(x,y)=\left(x^{(n)},y^{(n)}\right)},\\ h_1^{(n)} &= h_1(x^{(n)},y^{(n)}),\\ h_2^{(n)} &= h_2(x^{(n)},y^{(n)}),\end{aligned}$$

and

$$\begin{aligned}\mu_x^{(ni)} &= \sum_{j=1}^{N+L}\mu^{(ni)}\left.\frac{\partial\rho\left(x,y;x^{(j)},y^{(j)}\right)}{\partial x}\right|_{(x,y)=\left(x^{(i)},y^{(i)}\right)}\times\\ &\rho^{-1}\left(x^{(i)},y^{(i)};x^{(j)},y^{(j)}\right),\\ \mu_y^{(ni)} &= \sum_{j=1}^{N+L}\mu^{(ni)}\left.\frac{\partial\rho\left(x,y;x^{(j)},y^{(j)}\right)}{\partial y}\right|_{(x,y)=\left(x^{(i)},y^{(i)}\right)}\times\\ &\rho^{-1}\left(x^{(i)},y^{(i)};x^{(j)},y^{(j)}\right),\\ \mu^{(ni)} &= \sum_{j=1}^{N+L}\Psi^{(nj)}\rho^{-(ij)},\end{aligned}$$

$$\begin{aligned}\Psi^{(nj)} &= \lambda(x^{(n)},y^{(n)})\chi\left(x^{(n)},y^{(n)};x^{(j)},y^{(j)}\right) + \\ &\int_C\left[\Theta\left(x,y;x^{(n)},y^{(n)}\right)\frac{\partial\chi\left(x,y;x^{(j)},y^{(j)}\right)}{\partial n} - \right.\\ &\left.\chi\left(x,y;x^{(j)},y^{(j)}\right)\frac{\partial\Theta\left(x,y;x^{(n)},y^{(n)}\right)}{\partial n}\right]ds.\end{aligned}$$

Where

$$\rho^{(kl)} = 1 + r^2(x^{(k)},y^{(k)};x^{(l)},y^{(l)}) + r^3(x^{(k)},y^{(k)};x^{(l)},y^{(l)}),$$

and

$$\begin{aligned}\chi\left(x,y;x^{(m)},y^{(m)}\right) &= \frac{1}{4}r^2\left(x,y;x^{(m)},y^{(m)}\right) + \\ &\frac{1}{16}r^4\left(x,y;x^{(m)},y^{(m)}\right) + \\ &\frac{1}{25}r^5\left(x,y;x^{(m)},y^{(m)}\right).\end{aligned}$$

Function r is defined as

$$r(x,y;a,b) = \sqrt{(x-a)^2+(y-b)^2}.$$

By solving systems of linear algebraic Equations (5) and (6), numerical solutions at collocation points may be obtained. Using these solutions, numerical solution at any $(\xi,\eta)\in\Pi\cup\Lambda$ may also be obtained.

III. Result and Discussion

In this section, the DRM presented in Section II is applied to solve problems involving diffusion-convection equations. The first problem is a problem with analytical solution. This problem is used to investigate the accuracy of the DRM. The other problems are problems without analytical solution. These problems involving steady substance concentration range over shallow fluid path with a point source.

A. A problem with analytic solution

The diffusion-convection problem is given as follows:

$$s(x,y) = h_1(x,y)\frac{\partial Z(x,y)}{\partial x} + h_2(x,y)\frac{\partial Z(x,y)}{\partial y} - C\left(\nabla^2 Z(x,y)\right) \quad (7)$$

with

$$h_1(x,y) = y,\ h_2(x,y) = x,\ C = 1,$$

and

$$s(x,y) = 4xy,$$

defined over a square region with boundary conditions presented in Figure 1.

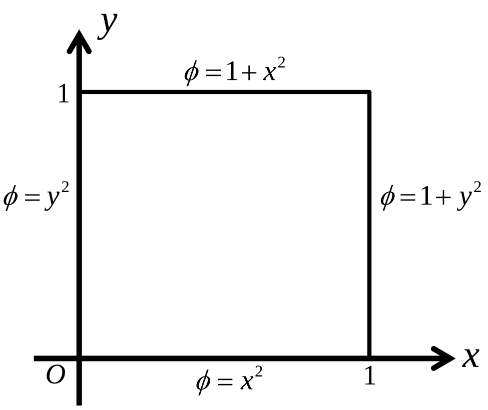

Fig. 1: Region and boundary conditions of diffusion-convection equation (7)

It is clear that Equation (7) subject to boundary conditions in Figure 1 has an analytical solution

$$\phi(x,y) = x^2 + y^2.$$

To solve the problem using the DRM, two sets of number boundary collocations and interior collocations are used, namely Set A and Set B. In Set A, 100 boundary collocation points and 100 interior collocation points were selected, while in Set B, 200 boundary collocation points and 225 interior collocation points were selected. The absolute errors resulted from Set A are in column e_A, and the absolute errors resulted from Set B are in column e_B. The results obtained are presented in Table I.

Table 1 shows numerical results obtained using DRM with Set A and Set B with corresponding absolute errors at selected points. From Table 1, it can be seen that numerical solutions obtained using the DRM are in good accuracy with the corresponding analytical solutions. The absolute errors obtained from Set B are, generally, smaller than those obtained from Set A. Moreover, the absolute errors resulted from Set A and Set B have maximum values of 0.0007 and 0.0001, respectively. These results show that Set B is better than Set A in accuracy.

TABLE I: Numerical and analytical solutions at selected points

Point	Analytic	Set A	Set B	e_A	e_B
$(0.2, 0.2)$	0.0800	0.08042	0.08008	0.00042	0.00008
$(0.4, 0.2)$	0.2000	0.20021	0.20002	0.00021	0.00002
$(0.6, 0.2)$	0.4000	0.40007	0.40004	0.00007	0.00004
$(0.8, 0.2)$	0.6800	0.68014	0.68004	0.00014	0.00004
$(0.2, 0.4)$	0.2000	0.20056	0.20008	0.00056	0.00008
$(0.4, 0.4)$	0.3200	0.32035	0.32008	0.00035	0.00008
$(0.6, 0.4)$	0.5200	0.52063	0.52005	0.00063	0.00005
$(0.8, 0.4)$	0.8000	0.80014	0.80007	0.00014	0.00007
$(0.2, 0.6)$	0.4000	0.40063	0.40006	0.00063	0.00006
$(0.4, 0.6)$	0.5200	0.52028	0.52004	0.00028	0.00004
$(0.6, 0.6)$	0.7200	0.72056	0.72001	0.00056	0.00001
$(0.8, 0.6)$	1.0000	1.00049	1.00002	0.00049	0.00002
$(0.2, 0.8)$	0.6800	0.68007	0.68009	0.00007	0.00009
$(0.4, 0.8)$	0.8000	0.80028	0.80007	0.00028	0.00007
$(0.6, 0.8)$	1.0000	1.00035	1.00002	0.00035	0.00002
$(0.8, 0.8)$	1.2800	1.28014	1.28003	0.00014	0.00003

B. Problems without analytical solutions

In this part, the DRM is applied to solve diffusion-convection equation problems to investigate the behavior of the spread of substances in a shallow straight path with a single source point. We consider a shallow straight path with length of L and width of W. The domain of the problems and the boundary conditions is shown in Figure 2.

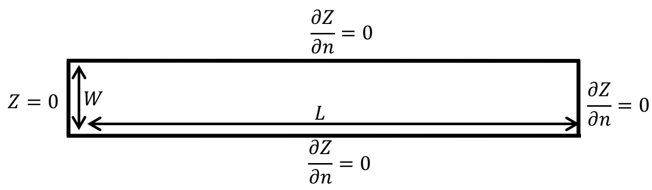

Fig. 2: Domain and boundary conditions of problems without analytical solutions.

It is assumed that at the upstream, at $x = 0$, the concentration of pollutant is zero ($Z = 0$). It is also assumed that there is no flux of pollutant flow across the riverside except from the point source. At line $x = L$, no pollutant flux flow across the line.

There are seven different cases considered in this study. The different cases studied are summarized in Table II.

TABLE II: Length, width, and flow velocity of different cases considered in this study.

Case	Length (L)	Width (W)	Flow velocity
Main case	96 m	24 m	1.5 m/s
Case 1	72 m	24 m	1.5 m/s
Case 2	120 m	24 m	1.5 m/s
Case 3	96 m	18 m	1.5 m/s
Case 4	96 m	30 m	1.5 m/s
Case 5	96 m	24 m	0.75 m/s
Case 6	96 m	24 m	3.0 m/s

We first solve the main case as the reference. The length, width, and flow velocity are 96 m, 24 m, and 1.5 m/s respectively. A point source is placed at point $(\frac{1}{4}L, \frac{1}{2}W)$ with pollutant flux of 200/107 gram/s and $C = 11.75$ m^2/s. To observe the effect of flow velocity to the distribution of pollutant, the flow velocities are varied as those in Case 5 and Case 6. Effects of length and width to the distribution of pollutant are examined by comparing the main case with Case 1, Case 2, Case 3, and Case 4.

Turbulent water flow on the path is modeled as the k-epsilon model system of equations as follows:

$$
\begin{aligned}
\frac{\partial v_x}{\partial x}+\frac{\partial v_y}{\partial y} &= 0\\
v_x\frac{\partial v_x}{\partial x}+v_y\frac{\partial v_x}{\partial y} &= -\frac{1}{\rho}\frac{\partial p}{\partial x}+\gamma\left(\frac{\partial^2 v_x}{\partial x^2}+\frac{\partial^2 v_x}{\partial y^2}\right)\\
v_x\frac{\partial v_y}{\partial x}+v_y\frac{\partial v_y}{\partial y} &= -\frac{1}{\rho}\frac{\partial p}{\partial y}+\gamma\left(\frac{\partial^2 v_y}{\partial x^2}+\frac{\partial^2 v_y}{\partial y^2}\right)\\
\frac{\partial}{\partial x}\left(\frac{v_t}{\sigma_k}\frac{\partial_k}{\partial x}\right) &= \epsilon-P_k\\
\frac{\partial}{\partial y}\left(\frac{v_t}{\sigma_k}\frac{\partial_k}{\partial y}\right) &= \epsilon-P_k\\
\frac{\partial}{\partial x}\left(\frac{v_t}{\sigma_\epsilon}\frac{\partial_\epsilon}{\partial x}\right) &= C_{\epsilon 2}\frac{\epsilon^2}{k}-C_{\epsilon 1}\frac{\epsilon}{k}P_k\\
\frac{\partial}{\partial y}\left(\frac{v_t}{\sigma_\epsilon}\frac{\partial_\epsilon}{\partial y}\right) &= C_{\epsilon 2}\frac{\epsilon^2}{k}-C_{\epsilon 1}\frac{\epsilon}{k}P_k
\end{aligned}
$$

where $v_t = c_\mu\frac{k^2}{\epsilon}$, $P_k=\frac{1}{2}v_t\left(\frac{\partial\vec{v_x}}{\partial y}+\frac{\partial\vec{v_y}}{\partial x}\right)$, $c_\mu = 0.09$, $c_{\mu 1} = 1.44$, $c_{\mu 2} = 1.92$, $\sigma_k = 1.00$, $\sigma_\epsilon = 1.30$, $\vec{v_i}$ is the shear stress respect to i direction, ρ is the density, γ is the kinematic viscosity and p is the pressure. For the cases considered the resulted velocity profiles are presented in Figure 3. These velocity profiles are obtained using *ANSYS 19.2*.

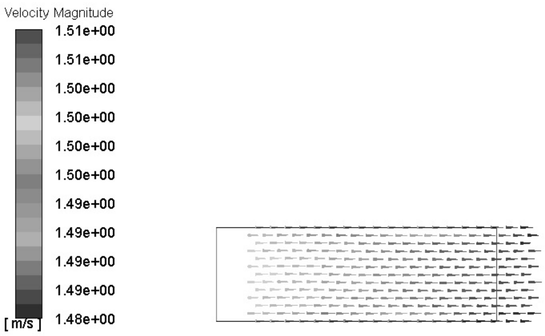

(a) Case 1

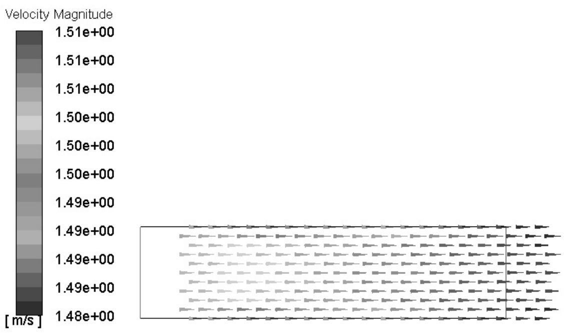

(b) Main Case

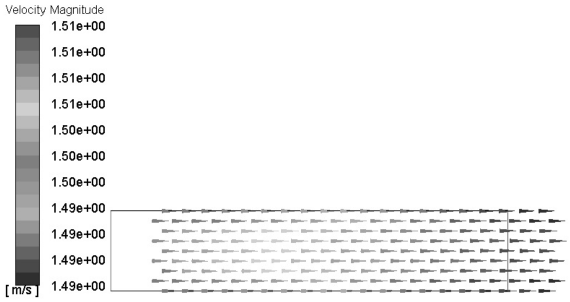

(c) Case 2

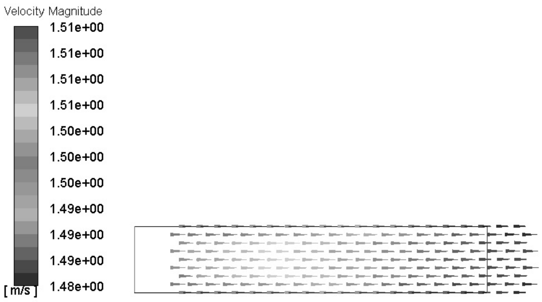

(d) Case 3

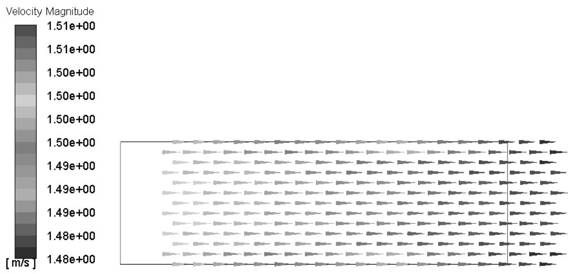

(e) Case 4

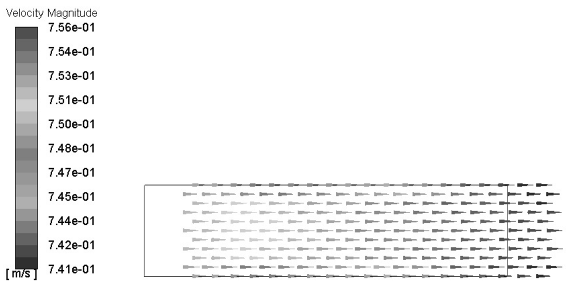

(f) Case 5

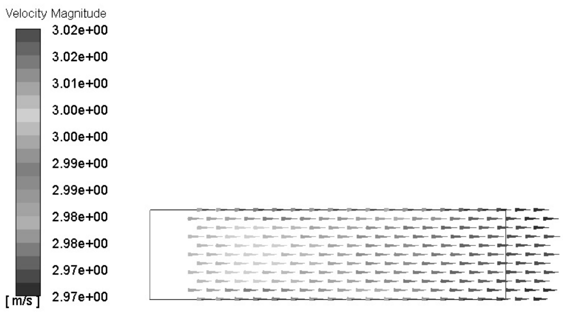

(g) Case 6

Fig. 3: Velocity profile for all cases generated by *ANSYS 19.2*.

To observe the effect of the number of boundary and interior collocations on DRM, several sets are selected to find a numerical solution for the Main Case. 200 boundary collocations and 200 interior collocations for Set C, 250 boundary collocations and 200 interior collocations for set D, and 250 boundary collocations and 250 interior collocations for Set E. The numerical results at some selected points from the three sets are shown in Table III.

TABLE III: Numerical solutions at selected points in Case 1

Point	Set C	Set D	Set E
(72.64, 12.00)	0.247818	0.248068	0.248068
(75.24, 12.00)	0.251528	0.251678	0.251728
(77.83, 12.00)	0.255186	0.255636	0.255286
(80.43, 12.00)	0.258759	0.259209	0.258859
(83.02, 12.00)	0.262195	0.262595	0.262495
(85.62, 12.00)	0.265433	0.265783	0.265783
(88.21, 12.00)	0.268414	0.268764	0.268614
(90.81, 12.00)	0.271117	0.271467	0.271567
(93.40, 12.00)	0.273569	0.273669	0.273819

It can be seen that the differences between solution obtained using Set C with the corresponding solutions obtained using Set D and Set E are less than 0.0005. Hence, for other cases we use Set C to implement the DRM. The numerical results are shown in Figure 4.

Furthermore, to analyze the behavior of the distribution of substances, lines l_1, l_2, and l_3 are selected from all cases, where $l_1 : x = \frac{1}{2}L$, $l_2 : x = \frac{3}{4}L$, and $l_3 : x = L$. The three lines are described in Figure 5.

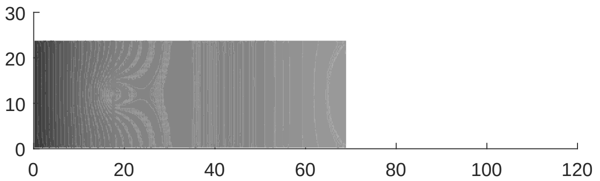

(a) Case 1

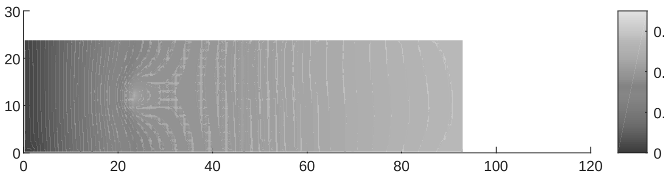

(b) Main Case

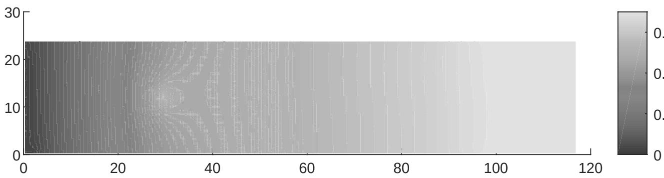

(c) Case 2

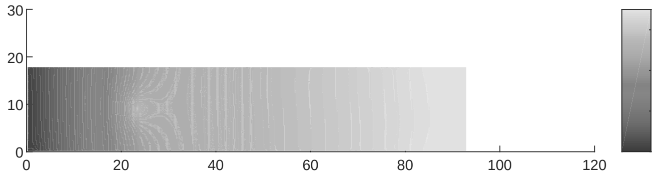

(d) Case 3

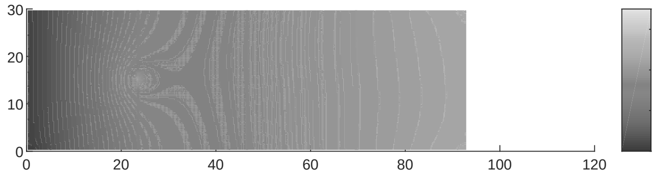

(e) Case 4

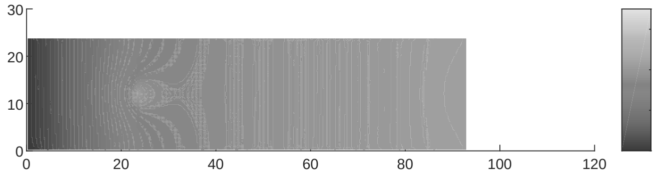

(f) Case 5

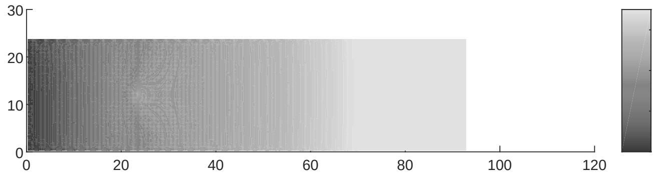

(g) Case 6

Fig. 4: Surface plot of substance concentration for all cases.

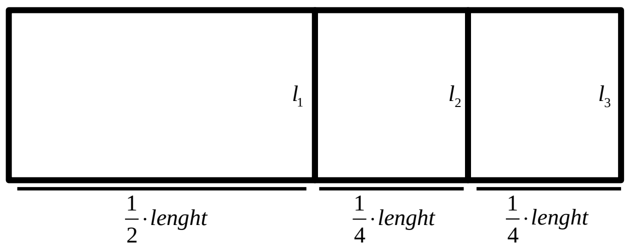

Fig. 5: Line l_1, l_2, and l_3 formulation.

Substance concentrations along lines, l_1, l_2, and l_3, from Case 1, Main Case, and Case 2 are shown in Figure 6. Figure 6 shows the relationship between the effect of path length and the behavior of the distribution of substance on the three lines. In Figure 6(a), it can be seen that the three cases show similar behavior. At a part close to the source point, the concentration of pollutant reaches the lowest value around 0.15 mg/litre for the path with length of 72 m and the highest value is 0.254 mg/litre for the path with length of 120 m. Similar results can also be observed at the area further from the source point. From these results, it can be concluded that the longer the path, the higher the substance concentration.

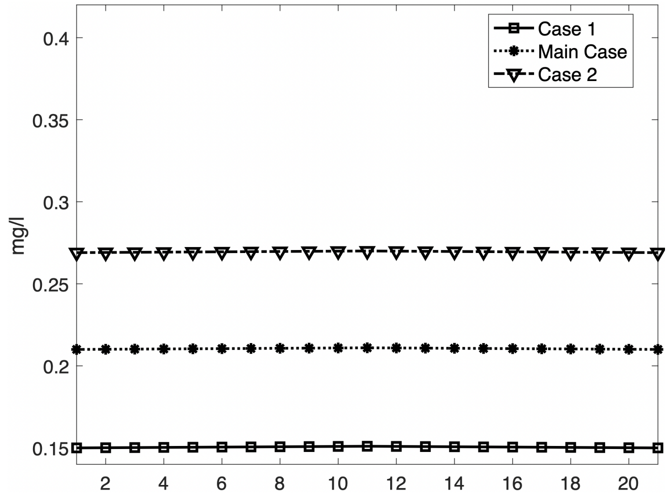

(a) Along line l_1

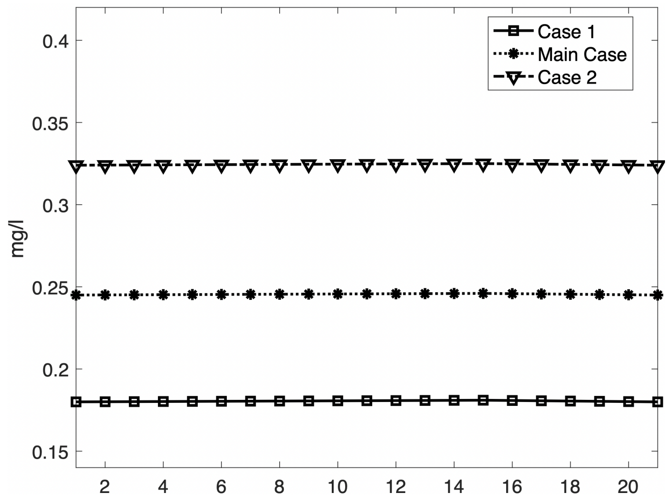

(b) Along line l_2

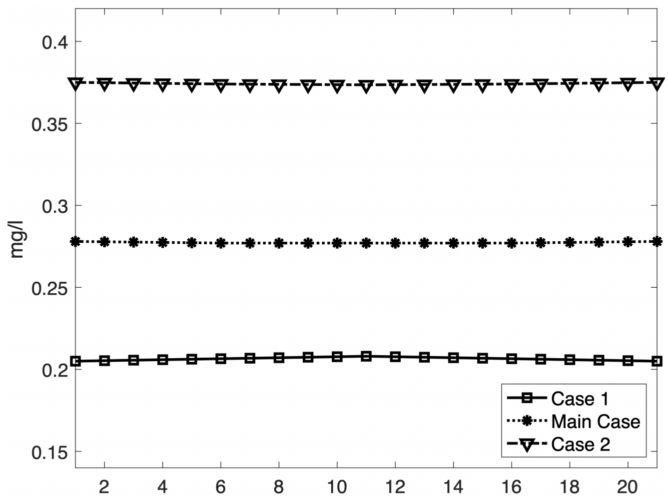

(c) Along line l_3

Fig. 6: Substance concentration along three lines for Case 1, Main Case and Case 2 based on path length.

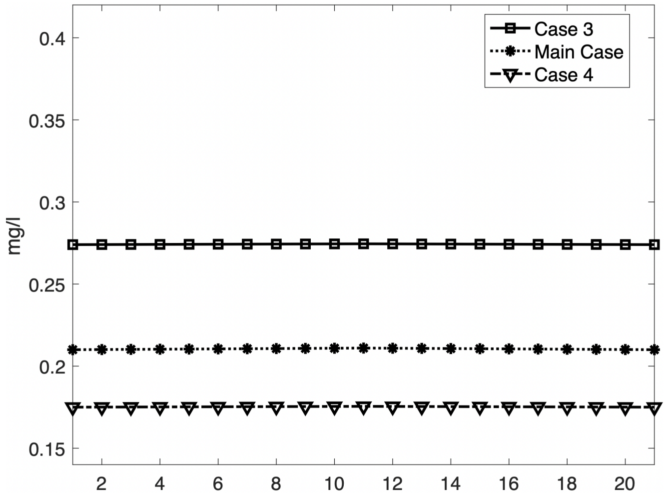

(a) Along line l_1

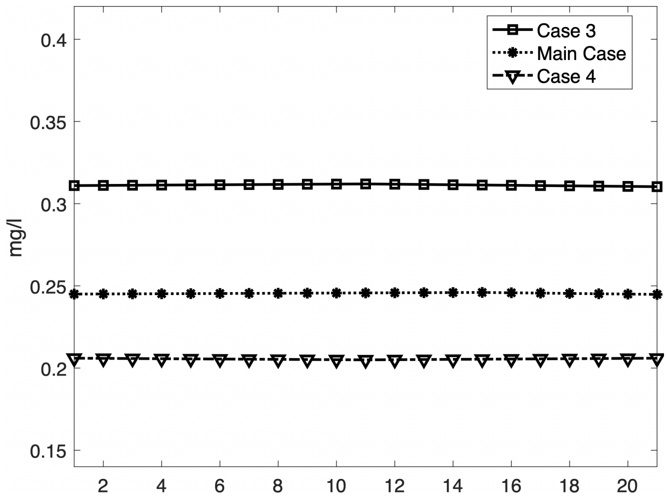

(b) Along line l_2

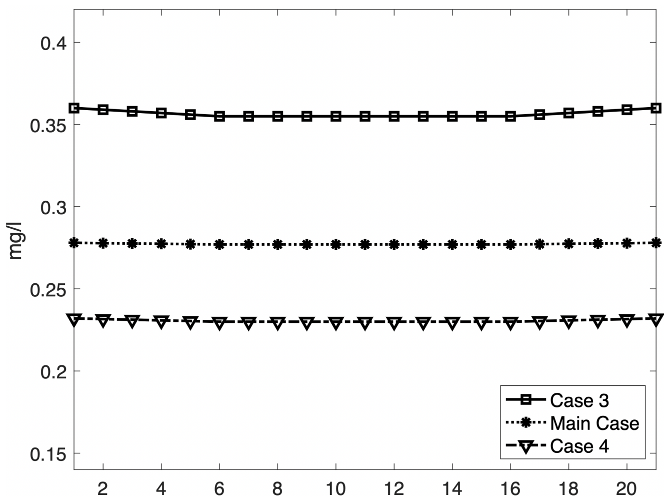

(c) Along line l_3

Fig. 7: Substance concentration along three lines for Case 3, Main Case and Case 4 based on path widht.

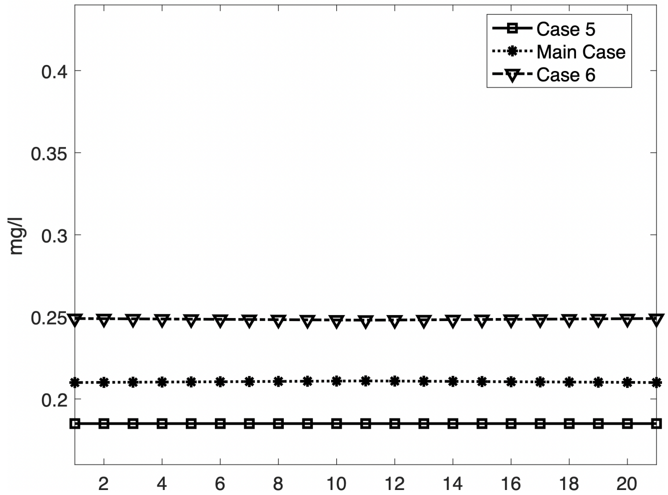

(a) Along line l_1

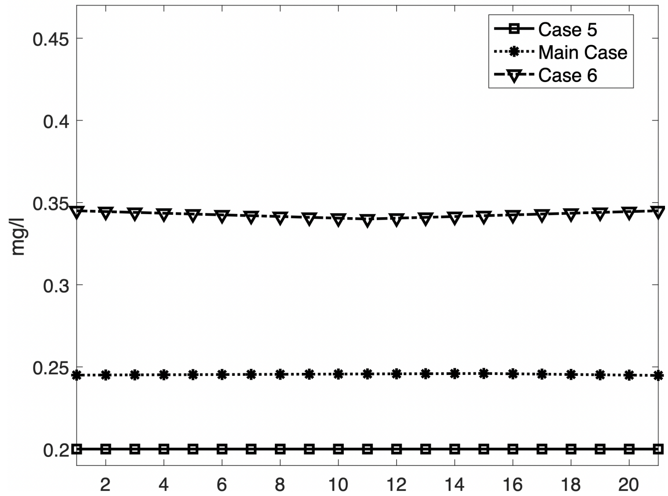

(b) Along line l_2

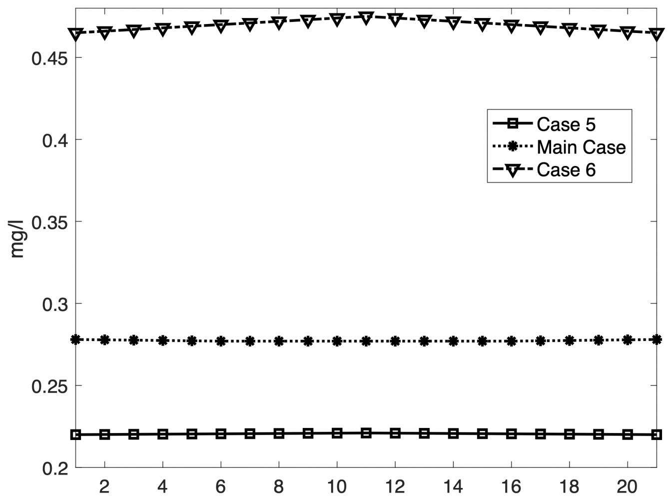

(c) Along line l_3

Fig. 8: Substance concentration along three lines for Case 5, Main Case and Case 6 based on flow velocity.

A comparison of the three cases along line l_2 is shown in Figure 6(b). It can be seen that the three cases show similar behavior to Figure 6(a) which is stable at a certain number. The part close to the source point has the lowest value around 0.156 mg/litre and the highest value is around 0.321 mg/litre. Meanwhile, the farthest part from the source point has the same results, the lowest value is around 0.156 mg/litre and the highest value is around 0.321 mg/litre. It can be concluded that the longer the path, the higher the concentration of the substance.

A comparison of the three cases along line l_3 is shown in Figure 6(c). It can be seen that for Case 1 it forms a concave downward line, while for Main Case and Case 2 it forms a downward convex line. This means that for Case 1 along line 13, the part that is close to the main stream will have a higher substance concentration value than the other part. On the other hand, for Main Case and Case 2 along line l_3, the part that is close to the main stream will have a lower substance concentration value than the other part. The part close to the source point has the lowest value around 0.205 mg/litre and the highest value is around 0.375 mg/litre. Meanwhile, the farthest part from the source point has the same results, the lowest value is around 0.205 mg/litre and the highest value is around 0.375 mg/litre. It can be concluded that the longer the path, the higher the concentration of the substance.

Furthermore, substance concentrations along three lines, l_1, l_2, and l_3 from Case 3, Main Case, and Case 4 are shown in Figure 7. This figure shows the relationship between the effect of the width of the path on the behavior of the distribution of substance on the three lines. In Figure 7(a), it can be seen that the three cases show similar behavior which is stable at a certain number. The part close to the source point has the lowest value around 0.155 mg/litre and the highest value is around 0.254 mg/litre. Meanwhile, the farthest part from the source point has the same results, namely the lowest value is around 0.155 mg/litre and the highest value is around 0.254 mg/litre. It can be concluded that the wider the path, the higher the concentration of the substance.

A comparison of the three cases along line l_2 is shown in Figure 7(b). It can be seen that the three cases show a similar behavior to Figure 7(a) which is stable at a certain number. The part close to the source point has the lowest value around 0.205 mg/litre and the highest value is about 0.312 mg/litre. Meanwhile, the farthest part from the source point has the same results, the lowest value is around 0.205 mg/litre and the highest value is 0.312 mg/litre. It can be concluded that the wider the path, the higher the concentration of the substance.

A comparison of the three cases along line l_3 is shown in Figure 7(c). It can be seen that for all three cases the line is convex downwards. This means that the three cases along line 1_3, the part that is close to the main stream will have a lower substance concentration value than the other part. The part close to the source point has the lowest value around 0.230 mg/litre and the highest value is about 0.351 mg/litre. Meanwhile, the farthest part from the source point has the same results, the lowest value is around 0.230 mg/litre and the highest value is around 0.351 mg/litre. It can be concluded that the wider the path, the higher the concentration of the substance.

Finally, substance concentration along three lines, l_1, l_2, and l_3, from Case 5, Main Case, and Case 6 are shown in Figure 8. This figure shows the relationship between the influence of current velocity on the behavior of the dispersion of substances on the three lines. In Figure 8(a), it can be seen that the three cases show similar behavior which is stable at a certain number. The part close to the source point has the lowest value around 0.156 mg/litre and the highest value is around 0.249 mg/litre. Meanwhile, the farthest part from the source point has the same results, namely the lowest value is around 0.156 mg/litre and the highest value is around 0.249 mg/litre. It can be concluded that the greater the flow velocity, the higher the concentration of the substance.

A comparison of the three cases along line l_2 is shown in Figure 8(b). It can be seen that the three cases show similar behavior to Figure 8(a) which is stable at a certain number. The part close to the source point has the lowest value around 0.20 mg/litre and the highest value is around 0.345 mg/litre. Meanwhile, the farthest part from the source point has the same results, the lowest value is around 0.20 mg/litre and the highest value is around 0.345 mg/litre. It can be concluded that the greater the flow velocity, the higher the concentration of the substance.

A comparison of the three cases along line l_3 is shown in Figure 8(c). It can be seen that for the three cases the values are stable at certain numbers except in Case 6 which forms a concave line downwards. This means that Case 6 along line l_3, the part that is close to the main stream will have a lower substance concentration value than the other part. The part close to the source point has the lowest value around 0.215 mg/litre and the highest value is around 0.475 mg/litre. Meanwhile, the farthest part from the source point has the same results, the lowest value is around 0.215 mg/litre and the highest value is around 0.475 mg/litre. From this it can be concluded that the greater the flow velocity, the higher the concentration of the substance.

The corresponding numerical results at selected points for graphs presented in Figure 6 - Figure 8 are presented in Table IV - Table XII. The results shown in the tables are similar to those presented in Figure 6 - Figure 8.

TABLE IV: Substance concentration along line l_1 for Case 1, Main Case and Case 2

Distance(m)	Case 1	Main Case	Case 2
1.0434	0.150549	0.208479	0.268623
2.0869	0.150582	0.208619	0.268759
3.1304	0.150594	0.208746	0.268895
4.1739	0.150615	0.208850	0.269006
5.2173	0.150647	0.208933	0.269095
6.2608	0.150685	0.209006	0.269174
7.3043	0.150727	0.209078	0.269256
8.3478	0.150766	0.209161	0.269355
9.3913	0.150798	0.209265	0.269482
10.4347	0.150821	0.209393	0.269640
11.4782	0.150832	0.209540	0.269823
12.5217	0.150830	0.209696	0.270021
13.5652	0.150816	0.209845	0.270213
14.6086	0.150791	0.209967	0.270377
15.6521	0.150761	0.210046	0.270496
16.6956	0.150727	0.210072	0.270554
17.7391	0.150695	0.210044	0.270549
18.7826	0.150669	0.209964	0.270483
19.8260	0.150652	0.209844	0.270365
20.8695	0.150643	0.209692	0.270208
21.9130	0.150612	0.209528	0.270043

TABLE V: Substance concentration along line l_2 for Case 1, Main Case and Case 2

Distance(m)	Case 1	Main Case	Case 2
1.0434	0.175696	0.241987	0.319970
2.0869	0.175657	0.242012	0.320078
3.1304	0.175622	0.242005	0.320120
4.1739	0.175586	0.241981	0.320136
5.2173	0.175555	0.241950	0.320140
6.2608	0.175531	0.241928	0.320153
7.3043	0.175515	0.241933	0.320195
8.3478	0.175505	0.241977	0.320282
9.3913	0.175498	0.242069	0.320422
10.4347	0.175495	0.242204	0.320610
11.4782	0.175493	0.242373	0.320834
12.5217	0.175494	0.242557	0.321071
13.5652	0.175496	0.242735	0.321296
14.6086	0.175501	0.242888	0.321484
15.6521	0.175510	0.243002	0.321617
16.6956	0.175525	0.243071	0.321688
17.7391	0.175548	0.243099	0.321703
18.7826	0.175579	0.243097	0.321673
19.8260	0.175614	0.243076	0.321614
20.8695	0.175649	0.243042	0.321525
21.9130	0.175687	0.242973	0.321342

TABLE VI: Substance concentration along line l_3 for Case 1, Main Case and Case 2

Distance(m)	Case 1	Main Case	Case 2
1.0434	0.202368	0.277418	0.376185
2.0869	0.202921	0.276482	0.375017
3.1304	0.203084	0.275992	0.374266
4.1739	0.203731	0.275263	0.373381
5.2173	0.203925	0.275267	0.373207
6.2608	0.204447	0.274765	0.372651
7.3043	0.204609	0.274940	0.372729
8.3478	0.204890	0.274647	0.372427
9.3913	0.205019	0.274816	0.372554
10.4347	0.205084	0.274740	0.372481
11.4782	0.205142	0.274815	0.372553
12.5217	0.205072	0.274934	0.372673
13.5652	0.204974	0.274907	0.372668
14.6086	0.204853	0.275168	0.372936
15.6521	0.204523	0.275095	0.372912
16.6956	0.204383	0.275452	0.373302
17.7391	0.203807	0.275450	0.373383
18.7826	0.203637	0.275912	0.373929
19.8260	0.202946	0.276148	0.374293
20.8695	0.202792	0.276832	0.375083
21.9130	0.202204	0.277257	0.375548

TABLE VII: Substance concentration along line l_1 for Case 2, Main Case and Case 3

Point	Case 3	Main Case	Case 4
0.7826	0.271375	0.208479	0.173866
1.5652	0.271445	0.208619	0.174006
2.3478	0.271523	0.208746	0.174134
3.1304	0.271587	0.208850	0.174240
3.9130	0.271638	0.208933	0.174320
4.6956	0.271685	0.209006	0.174387
5.4782	0.271737	0.209078	0.174449
6.2608	0.271804	0.209161	0.174526
7.0434	0.271894	0.209265	0.174621
7.8260	0.272009	0.209393	0.174737
8.6086	0.272146	0.209540	0.174858
9.3913	0.272295	0.209696	0.174989
10.1739	0.272442	0.209845	0.175110
10.9565	0.272572	0.209967	0.175184
11.7391	0.272671	0.210046	0.175213
12.5217	0.272730	0.210072	0.175187
13.3043	0.272744	0.210044	0.175082
14.0869	0.272715	0.209964	0.174929
14.8695	0.272650	0.209844	0.174740
15.6521	0.272559	0.209692	0.174522
16.4347	0.272468	0.209528	0.174289

TABLE VIII: Substance concentration along line l_2 for Case 2, Main Case and Case 3

Distance(m)	Case 3	Main Case	Case 4
1.0434	0.312501	0.241987	0.203185
2.0869	0.312577	0.242012	0.203162
3.1304	0.312595	0.242005	0.203116
4.1739	0.312594	0.241981	0.203043
5.2173	0.312588	0.241950	0.202969
6.2608	0.312590	0.241928	0.202904
7.3043	0.312614	0.241933	0.202870
8.3478	0.312673	0.241977	0.202881
9.3913	0.312770	0.242069	0.202946
10.4347	0.312904	0.242204	0.203060
11.4782	0.313065	0.242373	0.203218
12.5217	0.313237	0.242557	0.203399
13.5652	0.313403	0.242735	0.203568
14.6086	0.313544	0.242888	0.203727
15.6521	0.313647	0.243002	0.203831
16.6956	0.313708	0.243071	0.203898
17.7391	0.313730	0.243099	0.203928
18.7826	0.313723	0.243097	0.203932
19.8260	0.313695	0.243076	0.203916
20.8695	0.313646	0.243042	0.203884
21.9130	0.313513	0.242973	0.203846

TABLE IX: Substance concentration along line l_3 for Case 2, Main Case and Case 3

Distance(m)	Case 3	Main Case	Case 4
1.3043	0.356020	0.277418	0.233601
2.6086	0.355180	0.276482	0.232690
3.9130	0.354560	0.275992	0.232380
5.2173	0.353891	0.275263	0.231635
6.5217	0.353689	0.275267	0.231765
7.8260	0.353280	0.274765	0.231205
9.1304	0.353275	0.274940	0.231452
10.4347	0.353054	0.274647	0.231105
11.7391	0.353106	0.274816	0.231304
13.0434	0.353047	0.274740	0.231207
14.3478	0.353085	0.274815	0.231284
15.6521	0.353162	0.274934	0.231413
16.9565	0.353172	0.274907	0.231364
18.2608	0.353358	0.275168	0.231679
19.5652	0.353377	0.275095	0.231565
20.8695	0.353662	0.275452	0.231947
22.1739	0.353775	0.275450	0.231892
23.4782	0.354194	0.275912	0.232325
24.7826	0.354530	0.276148	0.232483
26.0869	0.355147	0.276832	0.233088
27.3913	0.355511	0.277257	0.233510

TABLE X: Substance concentration along line l_1 for Case 5, Main Case and Case 6

Distance(m)	Case 5	Main Case	Case 6
1.0434	0.182338	0.208479	0.248773
2.0869	0.182377	0.208619	0.248954
3.1304	0.182378	0.208746	0.248830
4.1739	0.182378	0.208850	0.248673
5.2173	0.182379	0.208933	0.248514
6.2608	0.182381	0.209006	0.248366
7.3043	0.182383	0.209078	0.248238
8.3478	0.182386	0.209161	0.248135
9.3913	0.182389	0.209265	0.248060
10.4347	0.182390	0.209393	0.248015
11.4782	0.182391	0.209540	0.248002
12.5217	0.182391	0.209696	0.248020
13.5652	0.182390	0.209845	0.248069
14.6086	0.182388	0.209967	0.248148
15.6521	0.182386	0.210046	0.248255
16.6956	0.182384	0.210072	0.248387
17.7391	0.182383	0.210044	0.248538
18.7826	0.182383	0.209964	0.248699
19.8260	0.182383	0.209844	0.248858
20.8695	0.182382	0.209692	0.248982
21.9130	0.182344	0.209528	0.248803

TABLE XI: Substance concentration along line l_2 for Case 5, Main Case and Case 6

Distance(m)	Case 5	Main Case	Case 6
1.0434	0.199270	0.241987	0.346113
2.0869	0.199241	0.242012	0.345881
3.1304	0.199230	0.242005	0.345639
4.1739	0.199218	0.241981	0.345363
5.2173	0.199205	0.241950	0.345076
6.2608	0.199192	0.241928	0.344801
7.3043	0.199180	0.241933	0.344557
8.3478	0.199170	0.241977	0.344354
9.3913	0.199162	0.242069	0.344201
10.4347	0.199156	0.242204	0.344102
11.4782	0.199153	0.242373	0.344058
12.5217	0.199152	0.242557	0.344070
13.5652	0.199153	0.242735	0.344138
14.6086	0.199157	0.242888	0.344260
15.6521	0.199163	0.243002	0.344433
16.6956	0.199170	0.243071	0.344649
17.7391	0.199180	0.243099	0.344899
18.7826	0.199190	0.243097	0.345167
19.8260	0.199201	0.243076	0.345431
20.8695	0.199211	0.243042	0.345666
21.9130	0.199239	0.242973	0.345895

TABLE XII: Substance concentration along line l_3 for Case 5, Main Case and Case 6

Distance(m)	Case 5	Main Case	Case 6
1.0434	0.216342	0.277418	0.475038
2.0869	0.216476	0.276482	0.476439
3.1304	0.216522	0.275992	0.477547
4.1739	0.216728	0.275263	0.479482
5.2173	0.216860	0.275267	0.480976
6.2608	0.217085	0.274765	0.482902
7.3043	0.217226	0.274940	0.484290
8.3478	0.217386	0.274647	0.485655
9.3913	0.217489	0.274816	0.486588
10.4347	0.217553	0.274740	0.487160
11.4782	0.217586	0.274815	0.487420
12.5217	0.217557	0.274934	0.487195
13.5652	0.217498	0.274907	0.486654
14.6086	0.217398	0.275168	0.485760
15.6521	0.217243	0.275095	0.484420
16.6956	0.217105	0.275452	0.483070
17.7391	0.216884	0.275450	0.481157
18.7826	0.216754	0.275912	0.479688
19.8260	0.216549	0.276148	0.477748
20.8695	0.216504	0.276832	0.476644
21.9130	0.216370	0.277257	0.475221

IV. CONCLUDING REMARKS

DRM has been successfully applied to the problem of a substance distribution in a straight path which has been modeled mathematically at steady state. Then DRM is used to check problem solutions with analytical solutions and without analytical solutions. Problems without analytical solutions are solved to determine the effect of length, width, and flow velocity on the distribution of substance.

When checking the results of numerical solutions to problems with analytical solutions, Set A with the number of boundary collocation points is 100 and the number of interior collocation points is 100, while Set B with the number of boundary collocation points is 200 and the number of interior collocations is 225. The result show that the absolute error of Set A and Set B are less than 0.0007 and 0.0001, respectively. Thus, the result of Set B is more accurate than Set A. So that it can be concluded that in general the more the number of collocation points, the more accurate the numerical calculation.

From the numerical results in the previous discussion, it can be confirmed that on selected three variables, length, width, and flow velocity, has almost similar behavior. In the problem of the distribution of substance in a straight path with turbulent flow, the greater the length, width, and flow velocity, the greater the concentration of substance that will be produced.

References

[1] N. Samec and L. Skerget, *Numerical modelling of pollutant dispersion in water systems*, vol 25. Slovenia: WIT Press, 1998.
[2] A. D. Polyanin, "Functional separable solutions of nonlinear convection-diffution equations with variable coefficients," Communications in Nonlinear Science and Numerical Simulation, vol. 73, pp. 379 - 390, 2019.
[3] V. F. Morales-Delgadoa, J. F. Gomez-Aguilar and M. A. Tanec-Hernandez,"Analytical solution of the time fractional diffusion equation and fractional covection-diffution equation,"Revista Mexicana de Fisica, vol. 65, pp. 82 - 88, 2019.
[4] W. Fajie, F. Chia-Ming, Z. Chuanzeng and L. Ji, "A Localized Space-Time Method of Fundamental Solutions for Diffusion and Convection-Diffusion Problems," Adv. Appl. Math. Mech., vol. 12, no. 4, pp. 940 - 958, 2020.
[5] Y. Xingxing, W. Fajie, H. Qingsong and Q. Xiang-Yun, "A novel space-time meshless method for nonhomogeneous convection-diffusion equations with variable coefficients," Applied Mathematics Letters, vol. 92, pp. 144 - 150, 2019.
[6] Z. Mengxin, Z. Weifeng and L. Ping, "Lattice Boltzmann method for general convection-diffusion equations: MRT model and boundary schemes," Journal of Computational Physics, vol. 389, pp. 147 - 163, 2019.
[7] I. Solekhudin, "Boundary interface water infiltration into layered soils using dual reciprocity methods," Engineering Analysis with Boundary Elements, vol. 119, pp. 280 - 292, 2020.
[8] H. Ji-Huan, "A simple approach to one-dimensional convection-diffusion equation and its fractional modification for E reaction arising in rotating disk electrodes," Journal of Electroanalytical Chemistry, vol. 389, pp. 147 - 163, 2019.
[9] D. Clements and M. Lobo, "A BEM for Time Dependent Infiltration from an Irrigation Channel," Engineering Analysis with Boundary Elements, vol. 34, pp. 1100 - 1104, 2010.
[10] I. Solekhudin and K.C. Ang, "A Laplace Transform DRBEM with a Predictor-Corrector Scheme for Time Dependent Infiltration from Periodic Channels with Root Water Uptake,"Engineering Analysis with Boundary Elements, vol. 50, pp. 141 - 147, 2015.
[11] I. Solekhudin, "A Numerical Method for Time-Dependent Infiltration from Periodic Trapezoidal Channels with Different Types of Root-Water Uptake," IAENG International Journal of Applied Mathematics, vol. 48, no. 1, pp. 84 - 89, 2018.
[12] Munadi, I. Solekhudin, Sumardi and A. Zulijanto, "Steady water flow from different types of single irrigation channel," JP Journal of Heat and Mass Transfer, vol. 16, no. 1, pp. 95 - 106, 2019.
[13] Munadi, I. Solekhudin, Sumardi and A. Zulijanto, "A Numerical Study of Steady Infiltration from a Single Irrigation Channel with an Impermeable Soil Layer," Engineering Letters, vol. 28, no.3, pp. 643 - 650, 2020.
[14] B.I. Yun and W.T. Ang, "A Dual Reciprocity Element Approach for Axisymmetric Nonlinear Time-Dependent Heat Conducyion in a Non-homogeneous Solid," Engineering Analysis with Boundary Elements, vol. 34, no. 8, pp. 697 - 706, 2010.
[15] N.Y. Ashar, "An Application of Dual Reciprocity Boundary Element Method on Calculation of Pollutant Concentration Range in Twinned Path with Laminar Water Flow," M.Sc. Thesis, Department of Mathematics, Universitas Gadjah Mada, Indonesia, 2020.
[16] N.Y. Ashar and I. Solekhudin, "A Numerical Study of Steady Pollutant Spread in Water from a Point Source," Engineering Letters, vol. 29, no.3, pp. 840 - 848, 2021
[17] I. Solekhudin, D. Purnama, N. H. Malysa and Sumardi, "Characteristics of water flow in heterogeneous soils," JP Journal of Heat and Mass Transfer, vol. 15, no. 3, pp. 597 - 608, 2019.